IEEE Access
Multidisciplinary | Rapid Review | Open Access Journal

Received March 13, 2021, accepted April 7, 2021, date of publication April 9, 2021, date of current version April 20, 2021.

Digital Object Identifier 10.1109/ACCESS.2021.3072332

Intelligent Energy-Based Modified Super Twisting Algorithm and Factional Order PID Control for Performance Improvement of PMSG Dedicated to Tidal Power System

YOUCEF BELKHIER[1], ABDELYAZID ACHOUR[1], NASIM ULLAH[2], RABINDRA N. SHAW[3], (Senior Member, IEEE), ZAHEER FAROOQ[4], ANEES ULLAH[5], AND ALI NASSER ALZAED[6]

[1]Laboratoire de Technologie Industrielle et de l'Information (LTII), Faculté de Technologie, Université de Bejaia, Bejaia 06000, Algeria
[2]Department of Electrical Engineering, College of Engineering, Taif University, Taif 21944, Saudi Arabia
[3]Department of Electronics and Communication Engineering, Galgotias University, Greater Noida 201308, India
[4]Department of Electrical Engineering, CECOS University Peshawar, Peshawar 25000, Pakistan
[5]Department of Electronic Engineering, University of Engineering Technology Peshawar (Abbottabad campus), Peshawar 25000, Pakistan
[6]Department of Architecture Engineering, College of Engineering, Taif University, Taif 21944, Saudi Arabia

Corresponding author: Youcef Belkhier (youcef.belkhier@univ-bejaia.dz)

This research work was supported by Taif University Researchers Supporting Project number (TURSP-2020/144), Taif University, Taif, Saudi Arabia.

ABSTRACT The majority of marine current conversion technologies are based on permanent magnet synchronous generators (PMSG) due to its numerous advantages such as high-power density, low cost, and favorable electricity production. However, nonlinear properties of the generator and parameter uncertainties, makes the controller design more than a simple challenge. This paper proposes a new adaptive passivity-based (PB) modified super twisting algorithm (PBSTA) for control performance improvement (low tracing errors, fast convergence response, robustness) of a PMSG based marine current energy conversion system under swell effect and parameter uncertainties. The proposed approach combines a new PB current control (PBCC) with a new adaptive modified super twisting algorithm through a fuzzy logic supervisor. A new adaptive fractional order PID (FO-PID) controller is introduced to design the desired dynamics of the system. The main contributions and motivation of this work include the extraction of maximum power from the tidal current, integrating it to the grid and making the closed loop system passive. This is possible by reshaping system energy and introducing a damping term that compensates the nonlinear terms by a damped way and not by cancellation. Two steps are needed to design the proposed controller: the first step includes the derivation of reference current based on the reference torque using adaptive FO-PID. In the second step, the overall control law is computed by the proposed PBSTA. The exponential stability and error convergence of the proposed controller are analytically proven. The developed controller is tested under parameter variations and it is compared to benchmark nonlinear control methods such as sliding mode. Extensive investigation under MATLAB/Simulink, demonstrates clearly that the proposed technique provides higher efficiency and robustness over the benchmark nonlinear control methods.

INDEX TERMS Tidal conversion system, permanent magnet synchronous generator, nonlinear control, passivity-based control.

I. INTRODUCTION

In the electric power sector, the world is seeking to significantly reduce its dependence on fossil fuels, which are characterized by high greenhouse gas emissions and unstable prices. At present, offshore tidal turbines are undergoing significant development due to the quality of the resources (depth and speed of the current), availability of abundant power (1.5 MW) and its more predictable behavior compared to wind and solar energies. In this area of research, the grid

The associate editor coordinating the review of this manuscript and approving it for publication was Qiuye Sun.

connected PMSG based tidal energy generation system is one of the most resent forms of renewable energy conservation problem to be investigated [1], [2].

Recently, various turbines based on permanent magnet synchronous generators (PMSG) have been developed to extract tidal energy. The most widely used technology to convert marine current energy consists of a tidal generator, PMSG, power converters and load. The topology has advantages such as ease of control, low cost, and clean energy. However, the power captured by this tidal conversion system highly depends on the applied control strategies. In fact, nonlinear properties of the generator, parameter uncertainties, and external disturbances, makes the controller design process very complicated. Furthermore, reactive power and DC-link over-voltage supports are the necessary conditions to connect the energy conversion system to the grid [3], [4].

In order to addresses the aforementioned issues, during the last decades extensive control theories have been investigated. A detailed review on the control strategies developed for PMSG based tidal energy conversion system is presented in [5]. For maximum power harnessing, a sliding mode control (SMC) strategy has been proposed in [6]. However, several factors such as changes in the parameters and sudden variations in the marine current velocity have not been taken into consideration. In [7], a novel active disturbance rejection control method (ADRC) is reported for the PMSG based marine energy conversion system discussed in [6]. The ADRC strategy treats the parameter uncertainties or changes as elements to be rejected which can be canceled during the control design. Compared to SMC and the classical PI control methods, the ADRC method [7] shows clear improvements in the performance of the power conversion system. In [8], a jaya-based sliding mode approach is reported to enhance the control performance of a tidal conversion system. The authors proposed an association of the tidal system with superconducting magnetic energy system (SCMES), for which, the jaya-based controller is applied. However, this association only improves the cost and maintenance time of the conversion system. In [9], a fuzzy sliding mode controller that adaptively extracts the maximum tidal power under swell effects is developed. However, the parameter changes and uncertainties have not been incorporated in the controller design. A magnetic equivalent circuit method-based second-order sliding mode is proposed in [10], however, external disturbances and parameter changes have not been considered in the design process. In order to extract the maximum power from the tidal current under large parametric uncertainties and nonlinearities, a nonlinear observer-based second-order SMC combined with a predictive control was developed in [11]. A linear quadratic controller is proposed in [12]. Using a real profile of the tidal current speed [13], a perturb and observe algorithm is proposed to track the maximum tidal power. Tilt-based fuzzy cascaded control combined with a new Q-network algorithm has been investigated by [14].

Nevertheless, in the aforementioned strategies, the PMSG physical properties are neglected. Thus, this paper investigates a new passivity-based modified super twisting algorithm (PBSTA) combined with a factional order PID controller (FO-PID) that maintain the PMSG operating at the optimal torque by tracking its velocity. Inherent advantages of the proposed strategy include the guaranteed robustness properties; the ensured stability and the nonlinear terms are not cancelled but compensated in a damped way. The proposed method makes the system passive, which is possible by introducing a damping term and reshaping its energy to regulate the physical variables to their desired values [15]. The system is decomposed into two interconnected subsystems with negative feedback. The new strategy controls the state dynamics of the electrical part, whiles the non-electrical dynamics are treated as a ''passive disturbance'', unlike the aforementioned nonlinear controls, which usually neglects the PMSG's mechanical part. To design the desired dynamics, a new adaptive fractional order PID controller via a fuzzy logic method is introduced, which enhances the robustness regardless of the external disturbances and parameter uncertainties of the PMSG. The proposed PBSTA is used to design the controller law, which ensures fast convergences of the measured signals toward their set values and guarantees high stability of the closed-loop system.

In [16], a PBC associated with a sliding-mode control (SMC) is proposed, as mentioned by the authors, the presented combined PBC-SMC control uses more than six fixed gains which is very difficult to determine their optimal values. In fact, as demonstrated by Zhou *et al.* in [7], fixed gains are very difficult to calculate if the control system exhibits parameter variations or uncertainties. In [17], a novel passivity-linear feedback control combined with a fuzzy logic controller is investigated. In [18], a new combined PBC is proposed, two approaches namely, standard passivity-based control and PI-passive controllers are presented. A passivity-based voltage control is developed in [4], however, as mentioned by the authors, the new controller shows a small sensitivity to the variation of the mechanical parameters. A passivity-based control with asymptotic convergence of the states is proposed [19]. The same system was considered in [20]. A PI-PBC is adopted to control the coupling phenomena of the PMSG. In [21], a PBC with a linear feedback controller is investigated for a PMSG based marine energy system, however, parameter uncertainties of the PMSG have not been considered. In [22], a robust adaptive passivity-based control scheme for a class of open-loop unstable nonlinear systems with actuator saturation in proposed. The authors in [23], investigated a passivity-based control combined with a fuzzy control and SMC by constructing a suitable fuzzy function. However, the controller design of the proposed combined strategy is complicated due to the mathematical.

This paper addresses the following two main objectives: controlling the PMSG to guarantee the extraction of maximum tidal power and integrate it to the grid. For this the new hybrid method is presented. The second task is to regulate the reactive power and the DC-link voltage to their references.

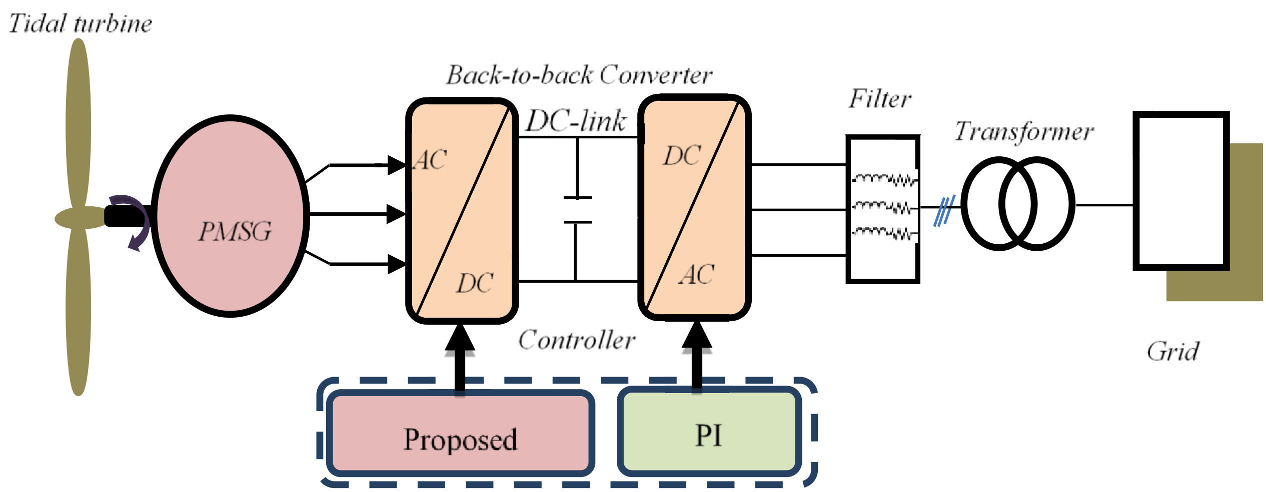

FIGURE 1. Studied system structure.

The disturbances include the nonlinear effects such as PMSG nonlinear friction and swell effect of the tidal velocity. A special attention is given to the generator side converter of the PMSG, as it's the bridge between the tidal turbine and the grid. Furthermore, the robustness against swell effect and parameter uncertainties has been taken into considerations.

The novelty and contribution of the present work are clearly summarized as follows:

- The new passivity-based modified super twisting algorithm combined with adaptive fractional order PID controller is investigated for performance improvement of a PMSG dedicated to marine current conversion system.
- The novel adaptive fractional PID controller via a fuzzy logic method as fuzzy gain supervisor is developed to design the desired dynamics. The fuzzy gain supervisor is used to adaptively adjust gains of the FO-PID which greatly enhance the robustness of the proposed approach against various uncertainties of PMSG.
- When designing the controller, the proposed strategy treats the mechanical characteristics as a passive disturbance, which is compensated in a damped way instead of direct cancellation.
- The global stability of the system and the exponential convergence of the current tracking errors have been analytically proven and further validated by extensive simulation results.

The rest of the paper is organized as follows: System description is established in section 2. Section 3 deals with the formulation of proposed hybrid control strategy. In section 4, GSC controller is discussed. Section 5, presents the numerical validation of the presented control strategy. Finally, the main conclusions are presented in section 6.

II. TIDAL GENERATOR MATHEMATICAL MODEL

The produced power via the generator is controlled by the proposed nonlinear observer-PBVC controller applied to the machine-side converter (see Fig. 1).

A. TIDAL POWER MODEL

The tidal power captured via the turbine and its related output torque, are expressed as follows [4], [7]:

$$P_m = \frac{1}{2}\rho C_p(\beta,\lambda)Av^3 \tag{1}$$

$$T_m = \frac{P_m}{\omega_t} \tag{2}$$

$$C_p(\beta,\lambda) = \frac{1}{2}\left(\frac{116}{\lambda_i} - 0.4\beta - 5\right)e^{-\left(\frac{21}{\lambda_i}\right)} \tag{3}$$

$$\lambda_i^{-1} = (\lambda + 0.08\beta)^{-1} - 0.035\left(1+\beta^3\right)^{-1} \tag{4}$$

$$\lambda = \frac{\omega_t R}{v} \tag{5}$$

From Eq. 4 and 5, β represents the pitch angle, v represents the tidal speed, λ denotes the tip-speed ratio, R represents the blades radius, ρ denotes the water density, ω_t denote the turbine speed, A represents the area of the blades, and C_p denotes the power coefficient.

B. PMSG MODEL

The adopted dq PSMG model is expessed bellow [4], [15]:

$$v_{dq} = R_{dq}i_{dq} + L_{dq}\dot{i}_{dq} + \psi_{dq}p\omega_m \tag{6}$$

$$J\dot{\omega}_m = T_m - T_e - f_{fv}\omega_m \tag{7}$$

$$T_e = \frac{2}{3}p\psi_{dq}^T i_{dq} \tag{8}$$

where, f_{fv} represents the viscous friction coefficient, $L_{dq} = \begin{bmatrix} L_d & 0 \\ 0 & L_q \end{bmatrix}$ represents dq inductances matrix, J is the moment of inertia, $i_{dq} = \begin{bmatrix} i_d \\ i_q \end{bmatrix}$ represents the stator current vector, T_e represents the electromagnetic torque, $\psi_{dq} = \begin{bmatrix} \psi_f \\ 0 \end{bmatrix}$ represents the flux linkages vector, $v_{dq} = \begin{bmatrix} v_d \\ v_q \end{bmatrix}$ represents

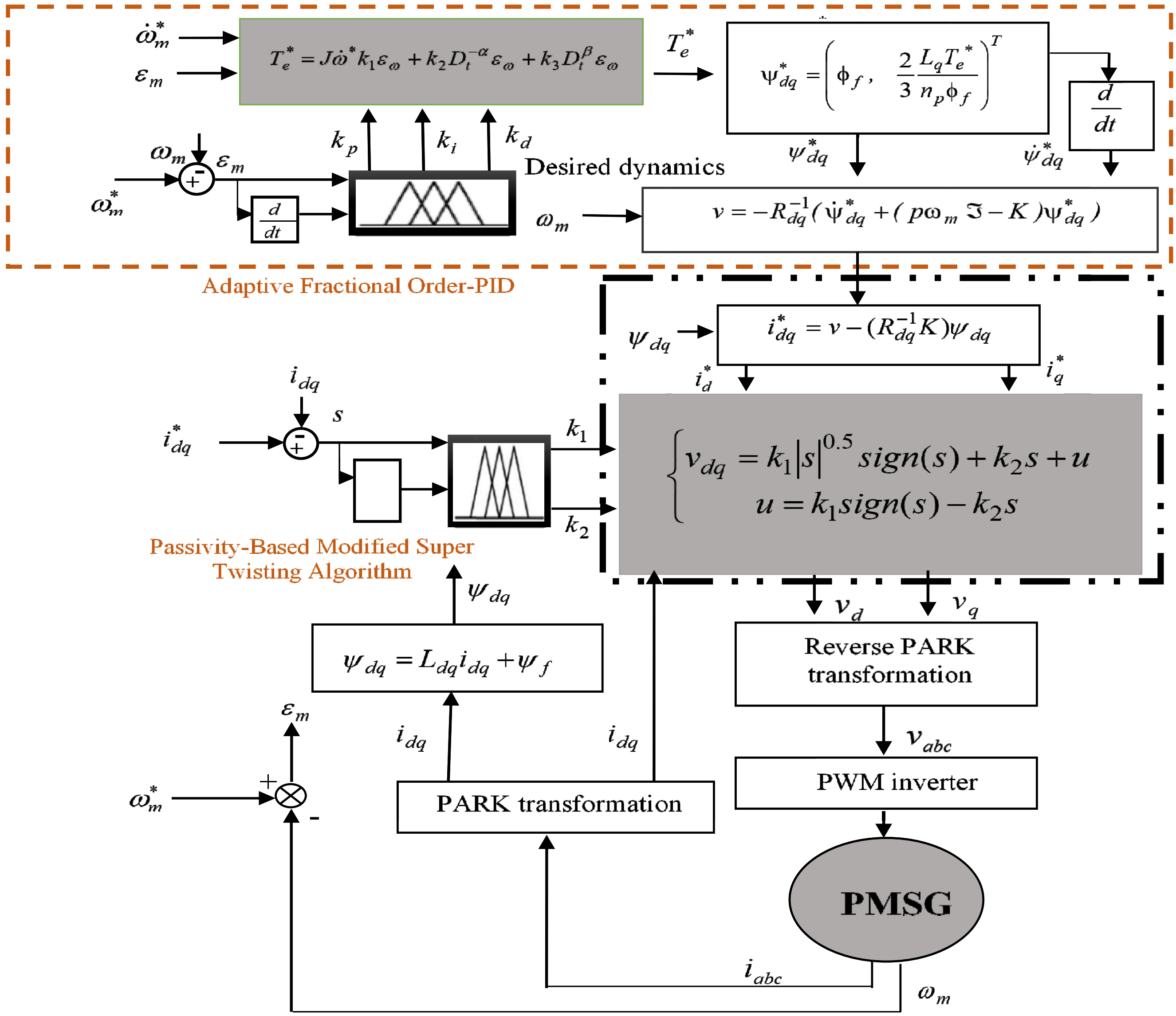

FIGURE 2. Proposed strategy design.

voltage stator vector, $R_{dq} = \begin{bmatrix} R_s & 0 \\ 0 & R_s \end{bmatrix}$ represents the stator resistance matrix.

III. PROPOSED CONTROLLER DESIGN PROCESS

The design of the new control strategy requires a number of steps: First, it is necessary to calculate an Euler-Lagrange model, to choose an appropriate input and output vectors such that the relationship between them is passive. Second, the system has to be decomposed into two interconnected subsystems with negative feedback. Finally, the last step consists to identify the non-dissipative terms in the system model. The controller design process is depicted in Fig. 2. Main idea for introducing the PBC control is to make the dynamics of the closed loop system passive and this is achieved by introducing a damping term and reshaping system's energy which compensates the nonlinear phenomena's in a damped way instead of direct cancellation. The controller design process is depicted in Fig. 2, in which, two main parts can be distinguished: The first step, is the computation of the reference electromagnetic torque, computed by the new adaptive FO-PID, and then from the reference torque, the desired current is obtained. The second part computes the control voltage using the proposed PBSTA controller.

A. PASSIVITY-BASED MODIFIED SUPER TWISTING ALGORITHM DESIGN

In [16], a proportional-integral (PI) control is proposed for the dq axis currents and to track its set vector $i^*_{dq} = \begin{bmatrix} i^*_d \\ i^*_q \end{bmatrix}$. However, as demonstrated by Zhou *et al.* in [7], fixed gains are very difficult to calculate if the control system exhibits parameter variations or uncertainties. Thus, the PBSTA controller is proposed to improve the robustness and resolve the problemes faced by the PI loops. Thus, the controller output voltages (v_{dq}) of the PMSG is computed as follows:

$$\begin{cases} v_{dq} = k_1 \left|s\right|^{0.5} sign(s) + k_2 s + u \\ u = k_1 sign(s) - k_2 s \end{cases} \tag{9}$$

$$s = \left(i_{dq}^{*} - i_{dq}\right) \tag{10}$$

where, $k_1 > 0$ and $k_2 > 0$. $s = \left(i_{dq}^{*} - i_{dq}\right)$, represent the sliding surface. The proposal is to find v_{dq} which ensures the convergence of the system dynamic. As indicated previously, fixed gains are very difficult to calculate if the system exhibits parameter variations. To overcome this problem, a fuzzy logic controller is used as gain supervisor. Then, the controller output v_{dq} is designed as shown in Fig. 3.

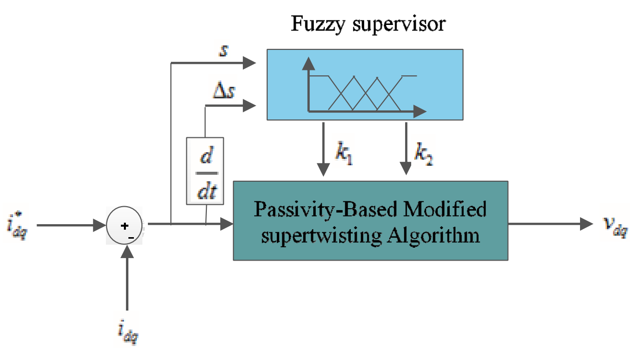

FIGURE 3. Controller law with the proposed adaptive PBSTA.

The fuzzy supervisor is used for the adaptation of the gains k_1 and k_2 of the PBSTA and thus, it solves the problem caused by imprecise parameters. The fuzzy inputs are chosen as the current error s and its derivative. The fuzzy control consists of three steps: In the first step the inputs are fuzzified, rules are formulated as a second step and finally the output is defuzzified. The types of the membership functions used are triangular and trapezoidal type uniformly distributed and symmetrical in the universe of discourse (see Fig. 4). The method of partitioning these functions is given according to Lee and Takagi [24] and Yubazaki *et al.* [25]. Their method is based on the idea of sharing the same parameter by several membership functions. The advantage of this method is that the number of parameters of the membership functions is significantly reduced. In Table 1, the linguistic variables corresponding to the inputs-outputs of the fuzzy gain scheduling are chosen as: Negative Big (NB), Negative Small (NS), Zero (Z), Positive Big (PB), and Positive Small (PS). The decision-making output is obtained using a Max-Min fuzzy inference where the crisp outputs are calculated by the center of gravity defuzzification method [26].

Remark 1: The choice of the fuzzy logic system to compute the gains of the modified super twisting algorithm is justified by the fact that fixed gains are complicated to calculate when the system is exposed to parameter uncertainties [26]. The reader is referred to [27] for more information about the super twisting control and its advantages.

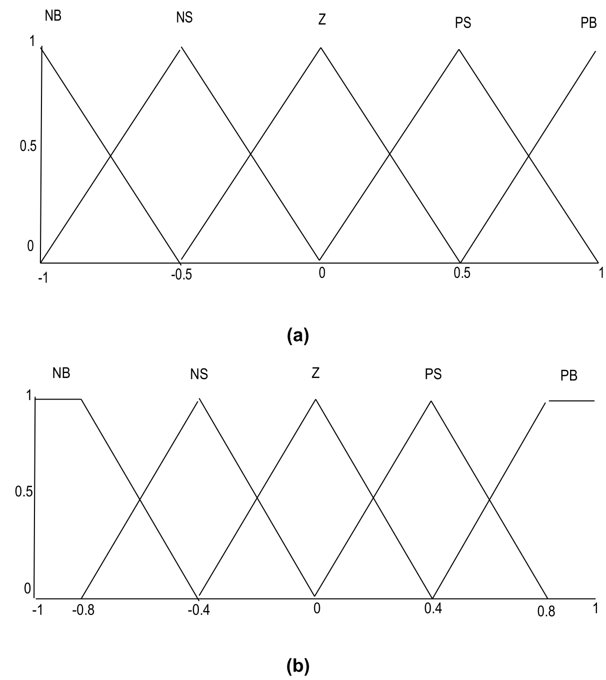

FIGURE 4. The fuzzy controller configuration. (a) Input membership function, (b) Output membership function.

TABLE 1. Fuzzy logic rules.

ε_ω \ $\Delta\varepsilon_\omega$	NB	NS	Z	PS	PB
NB	NB	NB	NS	NS	Z
NS	NB	NB	NS	Z	PS
Z	NS	NS	Z	PS	PS
PS	NS	Z	PS	PB	PB
PB	Z	PS	PS	PB	PB

B. PMSG PASSIVE FEEDBACK DECOMPOSTION

The PMSG input-output relationship for electrical part (6) can be formulated by the following expression:

$$\Sigma_e : V_e = \begin{bmatrix} v_{dq} \\ -\omega_m \end{bmatrix} \rightarrow Y_e = \begin{bmatrix} i_{dq} \\ T_m \end{bmatrix} \tag{11}$$

The mechanical part given in relation (7) can be expressed as follows:

$$\Sigma_m : V_m = (-T_e + T_m) \rightarrow Y_e = \frac{(-T_e + T_m)}{Js + f_{fv}} \tag{12}$$

Thus, the following lemma given below is introduced:

Lemma 1: According to the aforementioned conditions, the PMSG in the dq-model is divided into feedback interconnected two subsystems, i.e. electrical subsystem Σ_e and mechanical subsystem Σ_m.

Proof: From (11), total energy term H_e is given as follows:

$$H_e = \frac{1}{2} i_{dq}^T L_{dq} i_{dq} + \psi_{dq}^T i_{dq} \tag{13}$$

The time derivative of H_e along (6), yields the following expression:

$$\dot{H}_e = -i_{dq}^T R_{dq} i_{dq} + Y_e^T V_e + \frac{d}{dt}\left(\psi_{dq}^T i_{dq}\right) \tag{14}$$

Integrating both sides of (12) along $\left[\, 0 \; T_e \,\right]$, yields:

$$\underbrace{H_e(T_e) - H_e(0)}_{\substack{Stored\\Energy}} = \underbrace{-\int_0^{T_e} i_{dq}^T R_{dq} i_{dq} d\tau}_{\substack{Dissipated\\Energy}} + \underbrace{\int_0^{T_e} Y_e^T V_e d\tau + \left[\psi_{dq}^T i_{dq}\right]_0^{T_e}}_{\substack{Supplied\\Enerdy}} \tag{15}$$

where $H_e(T_e) \geq 0$ and $H_e(0)$ represents the initial energy stored. By integrating Eq. (15), a dissipation inequality is deduced, given as follows:

$$\int_0^{T_e} Y_e^T V_e d\tau \geq \lambda_{\min}\left\{R_{dq}\right\} \int_0^{T_e} \left\|i_{dq}\right\|^2 - \left(H_e(0) + \left[\psi_{dq}^T i_{dq}\right]_0^{T_e}\right) \tag{16}$$

where, $\|.\|$ represents the vector norm of the standard Euclidian.

From Eq. (16), it is established that Σ_e is passive. Then, from Σ_m, the transfer function $F_m(s)$ is expressed by the following expression:

$$F_m(s) = \frac{Y_m(s)}{V_m(s)} = \frac{1}{Js + f_{fv}} \tag{17}$$

It can be deduced that Σ_m is passive, since $F_m(s)$ is a strictly positive function. Thus, the PMSG model is decomposable into two passive sub systems which mean that the PMSG is passive.

C. DESIRED CURRENT CONTROLLER DESIGN

The aim is to design of the control inputs i_{dq}^* by proposed method that guarantees the convergence of the sliding surface. These results in the desired dynamics of the PMSG model are expressed as follows:

$$v_{dq} = R_{dq} i_{dq}^* + \dot{\psi}_{dq} + \psi_{dq} p \omega_m^* \tag{18}$$

$$J\dot{\omega}_m^* = T_m - T_e^* - f_{fv}\omega_m^* \tag{19}$$

$$T_e^* = \frac{2}{3} p \psi_{dq}^T i_{dq}^* \tag{20}$$

where, T_e^* denotes the desired electromagnetic torque and ω_m^* represents speed of the turbine (desired speed). Let us define the flux error given bellow:

$$e_f = \begin{bmatrix} e_{fd} \\ e_{fq} \end{bmatrix} = \psi_{dq}^* + \psi_{dq} \tag{21}$$

where, $\psi_{dq}^* = \left[\, \psi_d^* \; \psi_q^* \,\right]^T$ denotes the desired value of the flux linkages vector. By Substituting (21) in (19) and considering the Lyapunov function $V_L(e_f) = 0.5 e_f^T e_f$, the control signals i_{dq}^* which guarantees the asymptotic convergence of the error e_f, is expressed as expressed as follows:

$$i_{dq}^* = -\frac{1}{R_{dq}}\left(Ke_\psi - \left(\dot{\psi}_{dq}^* + p\omega_m \Im \psi_{dq}^*\right)\right) \tag{22}$$

where, $K = \begin{bmatrix} K_a & 0 \\ 0 & K_b \end{bmatrix}$, $K_a > 0$ and $K_b > 0$. The proof of the flux tracking error's exponential stability is given as follows: The time derivative along (19) of $V_L(e_f)$, yields the following relation:

$$\dot{V}_L(e_f) = -e_f^T K e_f \leq -\lambda_{\min}\{K\} \left\|e_f(t)\right\|^2, \forall t \geq 0 \tag{23}$$

$\lambda_{\min}\{K\}$ is the matrix and K represents the eigenvalues. The standard Euclidian norm's square of e_f is expressed as below:

$$\left\|e_f\right\|^2 = e_{fd}^2 + e_{fq}^2 \tag{24}$$

Combining (24) with $V_L(e_f)$, yields:

$$V_L(e_f) = 0.5 e_f^T e_f \leq \left\|e_f(t)\right\|^2, \forall t \geq 0 \tag{25}$$

Multiplying both sides of (25) with $(-\lambda_{\min}\{K\})$, yields:

$$(-\lambda_{\min}\{K\}) V_L(e_f) \geq (-\lambda_{\min}\{K\}) \left\|e_f(t)\right\|^2, \forall t \geq 0 \tag{26}$$

By combining (23) with (26), one obtains the following relation:

$$\dot{V}_L(e_f) \leq (-\lambda_{\min}\{K\}) V_L(e_f), \forall t \geq 0 \tag{27}$$

Integrating both sides of (27), gives:

$$V_L(e_f) \leq V_L(0) e^{-\lambda_{\min}\{K\} t}, \forall t \geq 0 \tag{28}$$

From (25) at t = 0, and multiplying it by $e^{-\lambda_{\min}\{K\} t}$, we get:

$$V_L(0) e^{-\lambda_{\min}\{K\} t} \leq \left\|e_f(0)\right\|^2 e^{-\lambda_{\min}\{K\} t} \tag{29}$$

Combining (29) with (28), yields:

$$V_L(e_f) \leq \left\|e_f(0)\right\|^2 e^{-\lambda_{\min}\{K\} t}, \forall t \geq 0 \tag{30}$$

From (25) and (30) it gives:

$$\left\|e_f(t)\right\|^2 \leq \left\|e_f(0)\right\|^2 e^{-0.5\lambda_{\min}\{K\} t} \tag{31}$$

Therefore, with a rate of convergence $\lambda_{\min}\{K\}$ the error e_f is exponentially decreasing, thus the system is asymptotically stable.

Remark 2: It is preferable to choose a high but limited value for this gain K, to permits a good convergence rate of the parameter $\lambda_{\min}\{K\}$ and to avoid divergence of i_{dq}. This limitation can be realized by simulation tests.

D. DESIRED TORQUE COMPUTATION USING THE PROPOSED ADAPTIVE FO-PID

The PMSG works at maximum torque if the direct current is maintained to zero. Thus, the flux ψ_d is reduced to the flux ϕ_f created by the permanent magnet. Then, the desired flux linkages are given as bellow:

$$\psi_{dq}^* = \begin{bmatrix}\psi_d^* \\ \psi_q^*\end{bmatrix} = \begin{bmatrix}\phi_f \\ L_d i_d^*\end{bmatrix} \tag{32}$$

From (32) and (20), the desired flux along q-axis is given by the following expression:

$$\psi_q^* = \frac{2}{3}\frac{L_q}{p\phi_f}T_e^* \tag{33}$$

Note that the controller law has two parts: The term that encloses the reference dynamics and the damping term that makes the system strictly passive.

The reference torque is derived from the mechanical dynamic equation (19), which is expressed by the following relation:

$$T_e^* = J\dot{\omega}_m^* + T_m - f_{fv}\varepsilon_m \tag{34}$$

Here $\varepsilon_m = \left(\omega_m^* - \omega_m\right)$ represents the speed error. The objective is to minimize the speed error between the PMSG and the marine current turbine. The above Eq. (39) shows clearly that T_e^* is dependent on two factors: It is open loop and the convergence property is a function of (J, f_{fv}) [4], [17]. To overcome the two factors, a fractional order fuzzy PID controller is adopted. It is well known that the robustness of the FO-PID is much better than the traditional PID and PI loops [17]. The inputs of the adaptive FO-PID fuzzy controller are ε_m and its derivative $\Delta\varepsilon_m$, and the outputs are the FO-PID control gains k_p, k_i and k_d. Then, Eq. (34) is expressed by the following form:

$$T_e^* = J\dot{\omega}_m^* - k_p\varepsilon_m - k_i D_t^{-\alpha}\varepsilon_m - k_d D_t^{\beta}\varepsilon_m \tag{35}$$

Here $K_p > 0, K_d > 0$ and $K_i > 0$, while $D_t^{-\alpha}$ represents fractional integration of order α and D_t^{β} represents fractional derivative with order β. For more information about the definition and theory of the FO-PID controller, the reader is referred to the following references [27], [29]. The design process of the fuzzy controller is the same as that used in section 3.A. The design of T_e^* by the adaptive FO-PID is illustrated by Fig. 5.

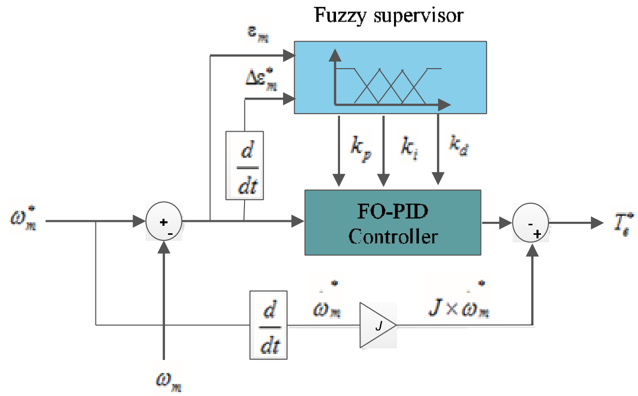

FIGURE 5. Desired torque with adaptive FO-PID.

IV. GLOBAL STABILITY OF THE PROPOSED STRATEGY

Lemma 2: The system is passive only if the dynamics expressed in (22) given by $\frac{1}{R_{dq}}\left(\dot{\psi}_{dq}^* + p\omega_m\Im\psi_{dq}^*\right)$ *and* ψ_{dq} *are considered as input and output.*

Proof: From (21), (22) and (6), the following equation is deduced:

$$\dot{\psi}_{dq} + \psi_{dq}p\omega_m = -R_{dq}\frac{1}{R_{dq}}\left(\dot{\psi}_{dq}^* + p\omega_m\Im\psi_{dq}^*\right) - Ke_f \tag{36}$$

Multiplying (36) by "$\frac{\psi_{dq}^T}{R_{dq}}$", yields the following expression:

$$\psi_{dq}^T\vartheta = -\frac{1}{2R_{dq}}\frac{d\left(\psi_{dq}^T\psi_{dq}\right)}{dt} - \psi_{dq}^T Ke_f \tag{37}$$

where, $\vartheta = \frac{1}{R_{dq}}\left(\dot{\psi}_{dq}^* + p\omega_m\Im\psi_{dq}^*\right)$. Since $\psi_{dq}^T\psi_{dq} = 0$, the term $p\omega_m R_{dq}^{-1}\psi_{dq}^T\psi_{dq}$ has no relation with the right hand side of Eq (37). From (31), e_f decreases exponentially. Then, the term $\psi_{dq}^T Ke_f$ is insignificant, and (37) become as bellow:

$$\psi_{dq}^T\vartheta = -\frac{1}{2R_{dq}}\frac{d\left(\psi_{dq}^T\psi_{dq}\right)}{dt} \tag{38}$$

Integration of (38), gives the following epression:

$$\int_0^t \psi_{dq}^T\vartheta\, dt = -\frac{1}{2R_{dq}}\left(\psi_{dq}^T\psi_{dq}\right)(t) + \frac{1}{2R_{dq}}\left(\psi_{dq}^T\psi_{dq}\right)(0) \tag{39}$$

Thus, by introducing $V_L(e_f)$, Eq. (39) can be rewritten as given below:

$$\int_0^t \psi_{dq}^T\vartheta\, dt = -\frac{1}{R_{dq}}V_L(t) + \frac{1}{R_{dq}}V_L(0) \tag{40}$$

Eq. 40, proves the passivity of the system while the energy balance of the system is independent of the term $p\omega_m R_{dq}^{-1}\psi_{dq}^T\psi_{dq}$, which has no influence on the stability of the system. Thus, the closed-loop system is globally stable.

V. PI CONTROLLER STRUCTURE OF THE GSC

To control reactive power support and stabilize the DC link voltage, the GSC convetrer controller is utilized. From [17], [20] the dynamics of GSC converter are expressed as follows:

$$\begin{bmatrix}V_{id} \\ V_{iq}\end{bmatrix} = R_f\begin{bmatrix}i_{df} \\ i_{qf}\end{bmatrix} + \begin{bmatrix}L_f\dot{i}_{df} - \omega L_f i_{qf} \\ L_f\dot{i}_{qf} - \omega L_f i_{df}\end{bmatrix} + \begin{bmatrix}V_{gd} \\ V_{gq}\end{bmatrix} \tag{41}$$

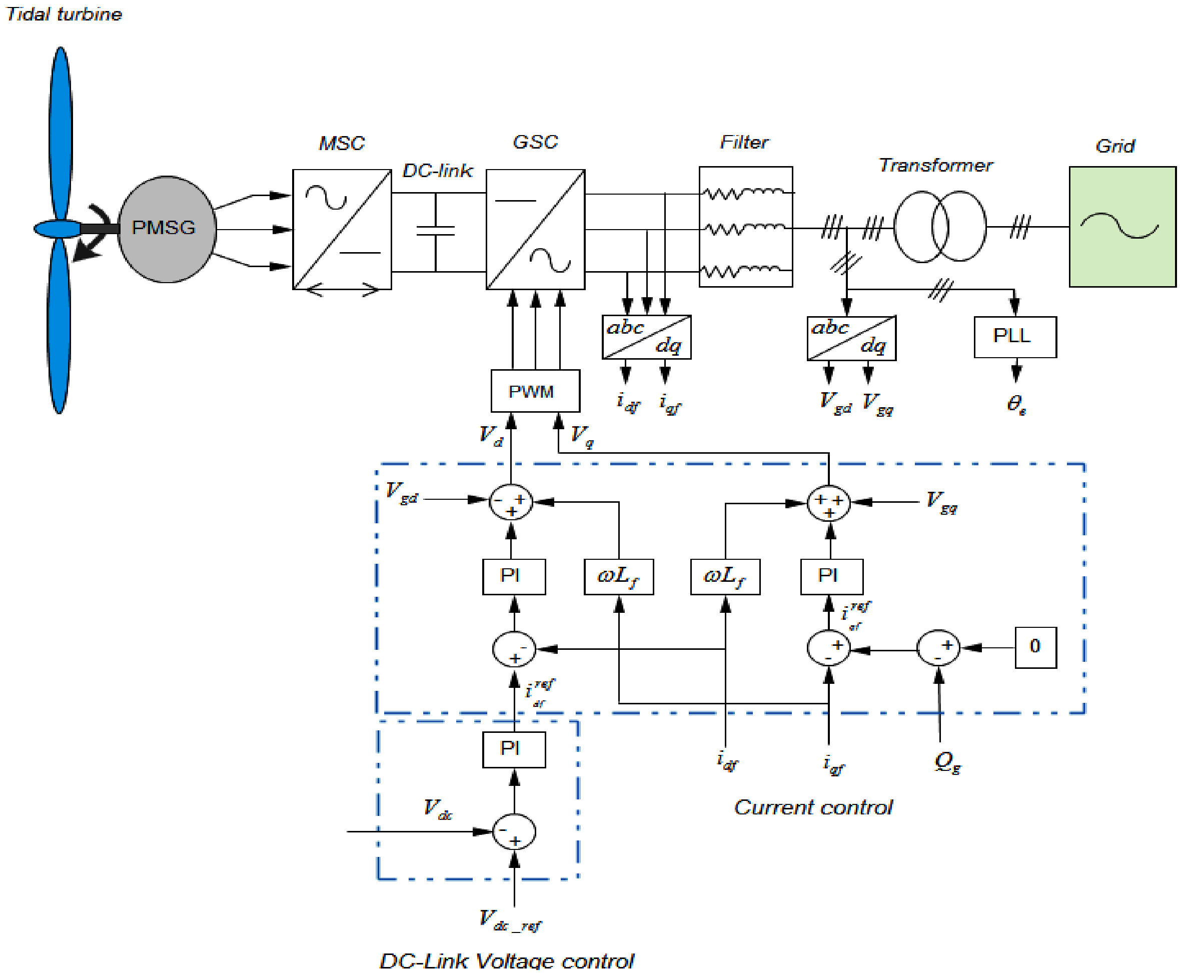

FIGURE 6. GSC PI controller structure.

From Eq. 41, ω is the grid frequency, V_{gd}, V_{gq} show the dq voltages, V_{id}, V_{iq} are the voltages measured at the inverter terminal, L_f represents filter inductance, i_{df} and i_{qf} are the dq component of the grid currents, and R_f gives resistance of the filter.

Dynamics of DC link are expressed as follows:

$$C\dot{V}_{dc} = \frac{3}{2}\frac{V_{gd}}{V_{dc}} i_{df} - i_{dc} \tag{42}$$

From Eq. 42, C is capacitance of DC link, V_{dc} represents voltage across DC link, and i_{dc} represents DC current.

Expressions for reactive and active powers are given by the following equations:

$$\begin{cases} P_g = \frac{3}{2} v_{gd} i_{df} \\ Q_g = \frac{3}{2} v_{gd} i_{qf} \end{cases} \tag{43}$$

The PI controller of the DC-link is expressed as follows:

$$i_{df}^{ref} = k_{dcp}\left(V_{dc\_ref} - V_{dc}\right) - k_{dci}\int_0^t \left(V_{dc\_ref} - V_{dc}\right) d\tau \tag{44}$$

where, $k_{dcp} > 0$ and $k_{dci} > 0$. The PI loops of the currents are given as follows:

$$v_{gd}^{PI} = k_{gp}^{d}\left(i_{df}^{ref} - i_{df}\right) - k_{gi}^{d}\int_0^t \left(i_{df}^{ref} - i_{df}\right) d\tau \tag{45}$$

$$v_{gq}^{PI} = k_{gp}^{q}\left(i_{qf}^{ref} - i_{qf}\right) - k_{gi}^{q}\int_0^t \left(i_{qf}^{ref} - i_{qf}\right) d\tau \tag{46}$$

where $k_{gp}^{d} > 0$, $k_{gi}^{d} > 0$, $k_{gp}^{q} > 0$ and $k_{gi}^{q} > 0$.

VI. NUMERICAL RESULTS

In this part, extensive numerical investigations are performed using Matlab/Simulink. System parameters are listed in Table 2. The reference reactive power is fixed to zero and the DC-link reference is set to 1150V. Using the pole location method, the damping parameters are given as follows: The PI gains of DC-link loop are chosen as: $k_{dcp} = 5$ and $k_{dci} = 500$. The damping gain is $K = 400$. Gains of the current loop controller are $k_{gp}^{d} = k_{gp}^{q} = 9$ and $k_{gi}^{d} = k_{gi}^{q} = 200$. The values of the two coefficients of FO-PID regulator are chosen as $\alpha = -0.79$ and $\beta = +0.55$. For more information about

TABLE 2. System parameters.

PMSG parameter	Value
Tidal density (ρ)	1024 kg/m^2
Tidal turbine radius (R)	10 m
Stator inductance (L_{dq})	0.3 mH
Stator resistance (R_s)	0.006 Ω
Stator inductance (L_{dq})	0.3 mH
Pole pairs number (p)	48
Flux linkage (ϕ_f)	1.48 Wb
Total inertia (J)	35000 kg.m^2
DC-link voltage (V_{dc})	1150 V
DC-link capacitor (C)	2.9 F
Grid-filter resistance (R_f)	0.3 pu
Grid-filter inductance (L_f)	0.3 pu

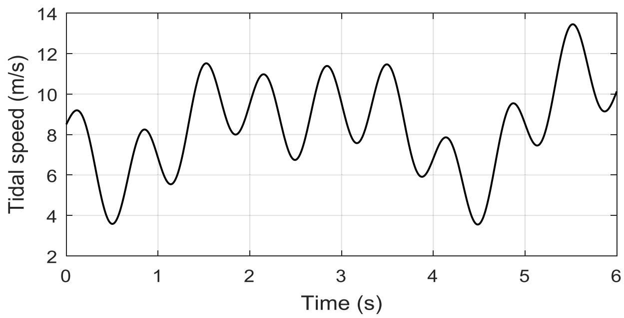

FIGURE 7. Tidal speed.

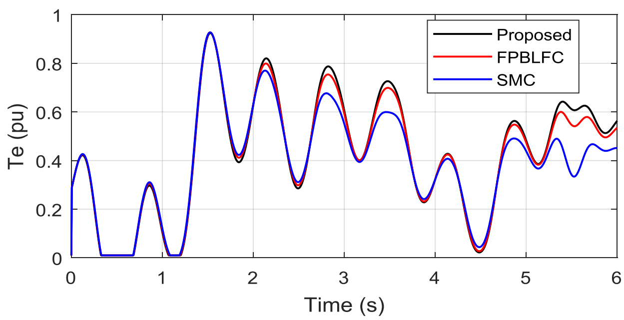

FIGURE 8. Electromagnetic torque.

the selection process of these two parameters, the reader is referred to [29]. The proposed strategy will be compared to the FPBLFC controller [17] and the second-order sliding mode control (SMC) controller [7]. Two scenarios are discussed: The first one deal with the testing of the proposed control under swell effect and with ideal parameters of the system. In the second scenario, the system is tested under swell effect and parameter uncertainties.

A. FIXED PARAMETERS ANALYSIS

The velocity of the tidal current with the considered swell effect is presented in Fig. 7. The tidal speed used in the simulation study varies between 3.9 m/s to 13.8 m/s. Fig. 8 shows the comparison of the electromagnetic torque of the PMSG generator produced as a result of the tidal velocity

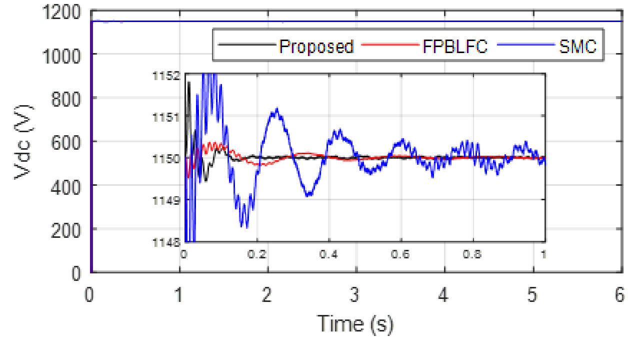

FIGURE 9. DC-link voltage.

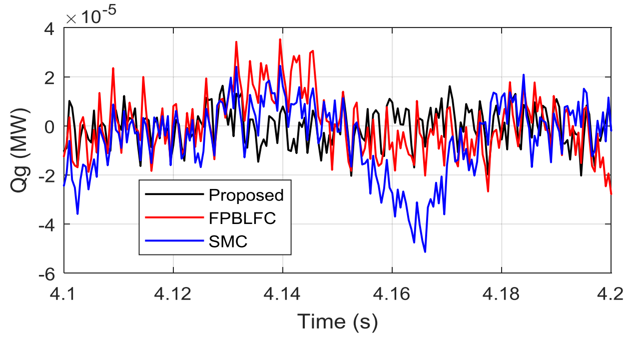

FIGURE 10. Zoom on reactive power.

of Fig. 7. One clearly concludes that under the influence by the swell effect the proposed strategy shows a higher electromagnetic torque as compared to the FPBLFC and SMC methods. From Fig.8 and in the time interval between t = 2-6 seconds, it is very obvious that the average generated electromagnetic torque with the proposed control scheme is higher as compared to the FPBLFC and SMC control methods. Fig. 9 shows the DC link voltage tracking response with FPBLFC, SMC and proposed control methods. From the presented results, a transient overshoot of +2 volts and undershoot of −2 volts is observed with SMC controllers. Similarly, a voltage overshoot of +0.5 volts and undershoot of −0.5 volts are observed with the FPBLFC control scheme. In case of proposed control method, lowest overshoot and undershoots are observed in the tracking response of the DC- link voltage. With the proposed control scheme, voltage overshoot of +0.3 volts and undershoot of −0.3 volts are recorded. Moreover, the proposed control ensures small oscillation and fast voltage tracking response. Fig. 10 shows the reactive power tracking comparison with SMC, FPBLFC and the proposed control schemes. From the presented results, a peak error of 0.5e-4 is observed with SMC, 0.4e-4 with the FPBLFC and 0.2e-4 with the proposed controller. Although the reactive power tracking errors are well bounded with all variants of control schemes, however, the proposed controller ensures the lowest tracking error and fast error tracking response. The active power response is shown in Fig. 11. From the presented results, it is obvious that in the time

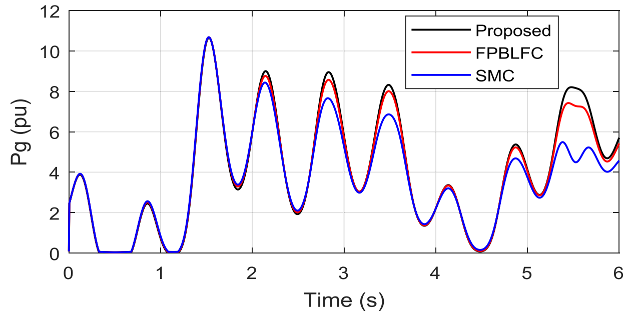

FIGURE 11. Active power.

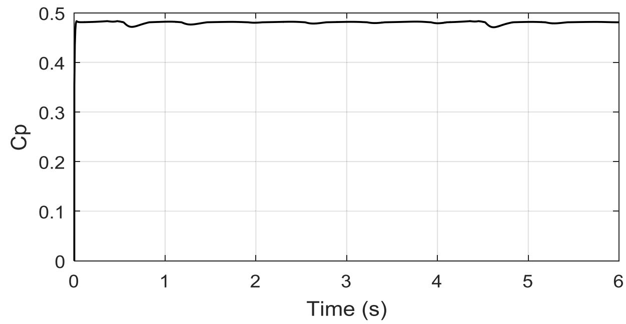

FIGURE 12. Power coefficient.

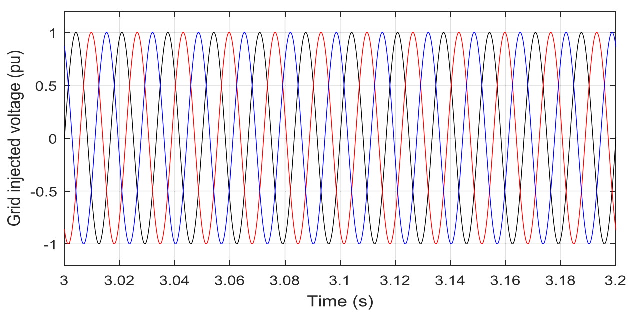

FIGURE 13. Generated voltage.

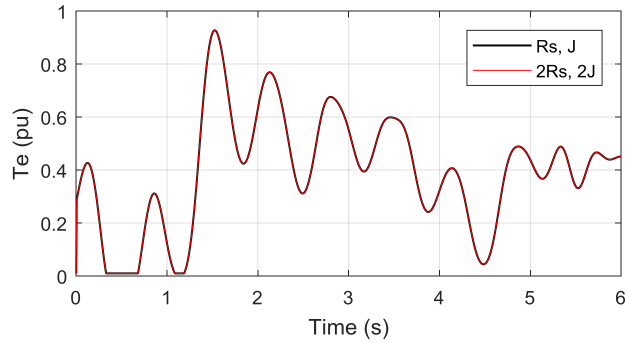

FIGURE 14. Torque response due to disturbances.

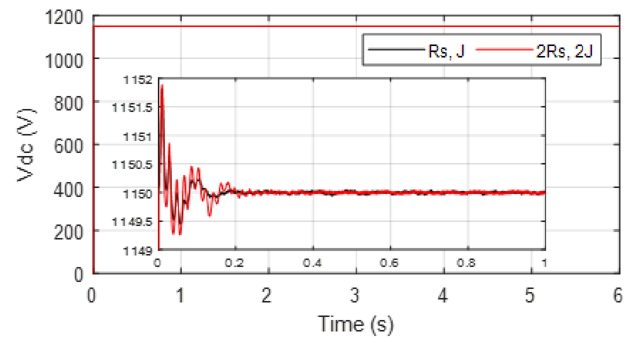

FIGURE 15. DC-link response due to disturbances.

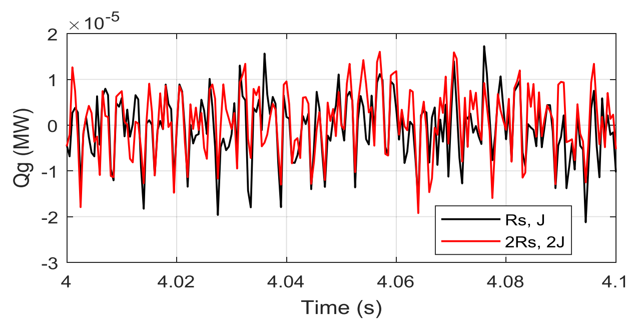

FIGURE 16. Reactive power response due to disturbances.

duration t = 2-6 seconds, the proposed controller integrates higher average active power to the grid under the swell effect. Fig. 12 shows the power coefficient of the turbine. Fig. 13 illustrates the grid injected voltage and from the presented results, it is obvious that the proposed control method ensures perfect sine voltage injection to the grid. In summary, and in comparison, to the other two benchmark nonlinear control methods, the proposed control scheme ensured lowest tracking errors, higher electromagnetic torque and active power with fast convergence of the states under swell effect.

B. ROBUSTENSS ANALYSIS

In the previous section, we presented fixed parameter analysis for the discussed control schemes under swell effect. In this section, the robustness of the proposed control scheme is tested under the effects of parameter variations and swell effects. Fig. 14 shows the response of the electromagnetic torque with the proposed control scheme under the effect of parameters variations. Simultaneous variations of +100% in the stator resistance and +100% in the total inertia are considered. From the presented results, it is obvious that the proposed controller efficiently compensates the parametric changes and the swell effect. Fig. 15 shows DC-link voltage regulation response with the proposed control scheme and under the above-mentioned disturbances. The presented results confirm the robustness of the proposed control scheme to the above-mentioned disturbances and the voltage regulation response is comparable to the fixed parameter test case. The measured error in DC-link voltage is approximately ±0.3 volts, which is comparable to test 1 (see Fig. 9). Fig. 16 confirms the robustness of the proposed strategy for tracking response of the reactive power to its reference value under the variations. From the presented results, it is observed that the recorded error is ±0.2e-4, which is approximately the

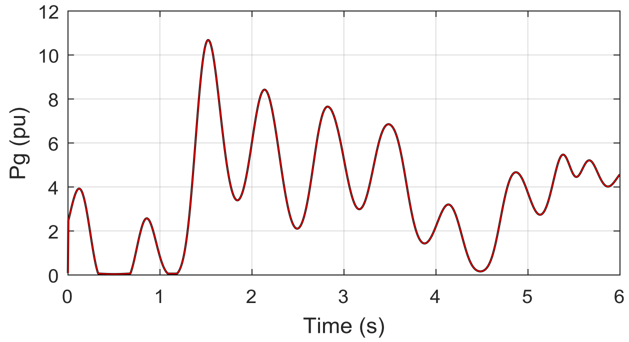

FIGURE 17. Active power response due to disturbances.

same as test case 1. Fig. 17 shows the active power transmitted to the grid under the effect of parameters variation and swell effect. It is obvious from the presented results that under these changes the active power is not influenced. In summary, under the effect of parametric uncertainty, the proposed control ensured stable operation of the DC-link voltage and the power transmitted to the grid. This further shows that the proposed controller can gain the stability performances with a constant power loads under parameter uncertainties and external disturbances studied in [30] and [31], for an efficient and secure electricity production [33], [34]. One can conclude after this test, that the proposed control firmly resists against simultaneous parameter changes and swell effect. Thus, in each scenario, the proposed strategy presents a higher dynamic response and robustness as compared to the other two nonlinear control methods. It also validates the mathematical demonstrations of the global stability and the exponential convergence of the error.

VII. CONCLUSION

In this paper, a novel intelligent passivity-based modified super twisting algorithm is presented for a PMSG assisted marine current conversion system. The proposed strategy is adopted to extract the maximum power from the tidal current, taking into account the entire dynamics of the PMSG when synthesizing the controller. The adaptive FO-PID is selected to guarantee fast response of the PMSG, and operate it at the optimal dynamics. Numerical simulations are presented under disturbances like swell effect and parameter changes. A comparative analysis of the system performance with proposed strategy is presented. All drawbacks of the conversion system are addressed and the control objectives are well achieved. The developed control strategy shows superior performance and higher robustness in comparison to the other nonlinear strategies. Future works will be focused on the experimental validation of the proposed controller.

REFERENCES

[1] G. Saini and R. P. Saini, "A review on technology, configurations, and performance of cross-flow hydrokinetic turbines," *Int. J. Energy Res.*, vol. 43, pp. 6639–6679, Jun. 2019.

[2] A. Benzerdjeb, B. Abed, H. Achache, M. K. Hamidou, and A. M. Gorlov, "Experimental study on blade pitch angle effect on the performance of a three-bladed vertical-axis Darrieus hydro turbine," *Int. J. Energy Res.*, vol. 43, no. 6, pp. 2123–2134, May 2019.

[3] M. Zhang, T. Wang, T. Tang, M. Benbouzid, and D. Diallo, "An imbalance fault detection method based on data normalization and EMD for marine current turbines," *ISA Trans.*, vol. 68, pp. 302–312, May 2017.

[4] Y. Belkhier and A. Achour, "Passivity-based voltage controller for tidal energy conversion system with permanent magnet synchronous generator," *Int. J. Control, Automat. Syst.*, vol. 19, pp. 1–11, Sep. 2020.

[5] P. Qian, B. Feng, H. Liu, X. Tian, Y. Si, and D. Zhang, "Review on configuration and control methods of tidal current turbines," *Renew. Sustain. Energy Rev.*, vol. 108, pp. 125–139, Jul. 2019.

[6] Z. Zhou, F. Scuiller, J. F. Charpentier, M. El Hachemi Benbouzid, and T. Tang, "Power smoothing control in a grid-connected marine current turbine system for compensating swell effect," *IEEE Trans. Sustain. Energy*, vol. 4, no. 3, pp. 816–826, Jul. 2013.

[7] Z. Zhou, S. Ben Elghali, M. Benbouzid, Y. Amirat, E. Elbouchikhi, and G. Feld, "Tidal stream turbine control: An active disturbance rejection control approach," *Ocean Eng.*, vol. 202, Apr. 2020, Art. no. 107190.

[8] A. M. Othman, "Enhancement of tidal generators by superconducting energy storage and Jaya-based sliding-mode controller," *Int. J. Energy Res.*, vol. 44, no. 14, pp. 11658–11675, Nov. 2020.

[9] Y.-J. Gu, X.-X. Yin, H.-W. Liu, W. Li, and Y.-G. Lin, "Fuzzy terminal sliding mode control for extracting maximum marine current energy," *Energy*, vol. 90, pp. 258–265, Oct. 2015.

[10] S. Toumi, E. Elbouchikhi, Y. Amirat, M. Benbouzid, and G. Feld, "Magnet failure-resilient control of a direct-drive tidal turbine," *Ocean Eng.*, vol. 187, Sep. 2019, Art. no. 106207.

[11] X. Yin and X. Zhao, "ADV preview based nonlinear predictive control for maximizing power generation of a tidal turbine with hydrostatic transmission," *IEEE Trans. Energy Convers.*, vol. 34, no. 4, pp. 1781–1791, Dec. 2019.

[12] R. Gaamouche, A. Redouane, I. El Harraki, B. Belhorma, and A. El Hasnaoui, "Optimal feedback control of nonlinear variable-speed marine current turbine using a two-mass model," *J. Mar. Sci. Appl.*, vol. 19, no. 1, pp. 83–95, Mar. 2020.

[13] S.-H. Moon, B.-G. Park, J.-W. Kim, and J.-M. Kim, "Maximum power-point tracking control using perturb and observe algorithm for tidal current generation system," *Int. J. Precis. Eng. Manuf.-Green Technol.*, vol. 7, no. 4, pp. 849–858, Jul. 2020.

[14] P. C. Sahu, R. Baliarsingh, R. C. Prusty, and S. Panda, "Novel DQN optimised tilt fuzzy cascade controller for frequency stability of a tidal energy-based AC microgrid," *Int. J. Ambient Energy*, 2020, doi: 10.1080/01430750.2020.1839553.

[15] A. Y. Achour, B. Mendil, S. Bacha, and I. Munteanu, "Passivity-based current controller design for a permanent-magnet synchronous motor," *ISA Trans.*, vol. 48, no. 3, pp. 336–346, Jul. 2009.

[16] B. Yang, T. Yu, H. Shu, Y. Zhang, J. Chen, Y. Sang, and L. Jiang, "Passivity-based sliding-mode control design for optimal power extraction of a PMSG based variable speed wind turbine," *Renew. Energy*, vol. 119, pp. 577–589, Apr. 2018.

[17] Y. Belkhier and A. Achour, "Fuzzy passivity-based linear feedback current controller approach for PMSG-based tidal turbine," *Ocean Eng.*, vol. 218, Dec. 2020, Art. no. 108156.

[18] W. Gil-Gonzalez, A. Garces, and O. B. Fosso, "Passivity-based control for small hydro-power generation with PMSG and VSC," *IEEE Access*, vol. 8, pp. 153001–153010, 2020.

[19] F. Mancilla-David and R. Ortega, "Adaptive passivity-based control for maximum power extraction of stand-alone windmill systems," *Control Eng. Pract.*, vol. 20, no. 2, pp. 173–181, Feb. 2012.

[20] R. Cisneros, F. Mancilla-David, and R. Ortega, "Passivity-based control of a grid-connected small-scale windmill with limited control authority," *IEEE J. Emerg. Sel. Topics Power Electron.*, vol. 1, no. 4, pp. 247–259, Dec. 2013.

[21] B. Yang, T. Yu, H. Shu, D. Qiu, Y. Zhang, P. Cao, and L. Jiang, "Passivity-based linear feedback control of permanent magnetic synchronous generator-based wind energy conversion system: Design and analysis," *IET Renew. Power Gener.*, vol. 12, no. 9, pp. 981–991, Jul. 2018.

[22] M. Hosseinzadeh and M. J. Yazdanpanah, "Robust adaptive passivity-based control of open-loop unstable affine non-linear systems subject to actuator saturation," *IET Control Theory Appl.*, vol. 11, no. 16, pp. 2731–2742, Nov. 2017.

[23] R. Subramaniam and Y. H. Joo, "Passivity-based fuzzy ISMC for wind energy conversion systems with PMSG," *IEEE Trans. Syst., Man, Cybern., Syst.*, vol. 51, no. 4, pp. 2212–2220, Apr. 2019.

[24] A. Michael and H. Takagi, "Dynamic control of genetic algorithms using fuzzy logic techniques," in *Proc. Int. Conf. Genetic Algorithms*, San Mateo, CA, USA, 1993, pp. 76–83.

[25] N. Yubazaki, M. Otani, T. Ashida, and K. Hirota, "Dynamic fuzzy control method and its application to positioning of induction motor," in *Proc. IEEE Int. Conf. Fuzzy Systems. Int. Joint Conf., 4th IEEE Int. Conf. Fuzzy Syst., 2nd Int. Fuzzy Eng. Symp.*, Tokyo, Japan, Mar. 1995, pp. 1095–1102.

[26] K. Ghefiri, A. Garrido, E. Rusu, S. Bouallègue, J. Haggège, and I. Garrido, "Fuzzy supervision based-pitch angle control of a tidal stream generator for a disturbed tidal input," *Energies*, vol. 11, no. 11, p. 2989, Nov. 2018.

[27] I. Sami, S. Ullah, Z. Ali, N. Ullah, and J.-S. Ro, "A super twisting fractional order terminal sliding mode control for DFIG-based wind energy conversion system," *Energies*, vol. 13, no. 9, p. 2158, May 2020.

[28] H. Chen, W. Xie, X. Chen, J. Han, N. Aït-Ahmed, Z. Zhou, T. Tang, and M. Benbouzid, "Fractional-order PI control of DFIG-based tidal stream turbine," *J. Mar. Sci. Eng.*, vol. 8, no. 5, p. 309, Apr. 2020.

[29] N. Ullah, I. Sami, M. S. Chowdhury, K. Techato, and H. I. Alkhammash, "Artificial intelligence integrated fractional order control of doubly fed induction generator-based wind energy system," *IEEE Access*, vol. 9, pp. 5734–5748, 2021.

[30] R. Wang, Q. Sun, W. Hu, Y. Li, D. Ma, and P. Wang, "SoC-based droop coefficients stability region analysis of the battery for stand-alone supply systems with constant power loads," *IEEE Trans. Power Electron.*, vol. 36, no. 7, pp. 7866–7879, Jul. 2021.

[31] W. Rui, S. Qiuye, M. Dazhong, and H. Xuguang, "Line impedance cooperative stability region identification method for grid-tied inverters under weak grids," *IEEE Trans. Smart Grid*, vol. 11, no. 4, pp. 2856–2866, Jul. 2020.

[32] R. Wang, Q. Sun, D. Ma, and Z. Liu, "The small-signal stability analysis of the droop-controlled converter in electromagnetic timescale," *IEEE Trans. Sustain. Energy*, vol. 10, no. 3, pp. 1459–1469, Jul. 2019, doi: 10.1109/TSTE.2019.2894633.

[33] W. Hu, C. Ruan, H. Nian, and D. Sun, "Zero-sequence current suppression strategy with common-mode voltage control for open-end winding PMSM drives with common DC bus," *IEEE Trans. Ind. Electron.*, vol. 68, no. 6, pp. 4691–4702, Jun. 2021, doi: 10.1109/TIE.2020.2988221.

YOUCEF BELKHIER received the master's degree in automatic from the University of Bejaia, Algeria, in 2017, where he is currently pursuing the Ph.D. degree. His research interests include electrical machines design, control, and renewable energy systems.

ABDELYAZID ACHOUR received the Magister degree from the Polytechnic Military School (EMP), Algeria, in 1999, and the Ph.D. degree from Bejaia University, Algeria, in 2009. He is currently an Associate Professor of automatic and electrical engineering with the Electrical Engineering Department, University of Bejaia. His research interest includes electrical machines design and control.

NASIM ULLAH received the Ph.D. degree in mechatronic engineering from Beihang University, Beijing, China, in 2013. From September 2006 to 2010, he was a Senior Design Engineer with IICS, Pakistan. He is currently working as an Associate Professor of electrical engineering with Taif University, Saudi Arabia. His research interests include renewable energy, flight control systems, integer and fractional order modeling of dynamic systems, integer/fractional order adaptive robust control methods, fuzzy/NN, hydraulic and electrical servos, epidemic, and vaccination control strategies.

RABINDRA N. SHAW (Senior Member, IEEE) worked as a University Examination Coordinator, MOOCs Coordinator, University Conference Coordinator and In Charge. COE PE&CEI, he has more than 11 years teaching experience in leading institutes, like Motilal Nehru National Institute of Technology, Allahabad, India, Jadavpur University, and others in UG and PG level. He is currently holding the position of Faculty In-Charge International Affairs and Collaborations at Galgotias University, India.

ZAHEER FAROOQ received the B.Sc. and M.Sc. degrees in electrical engineering from the University of Science and Technology, Peshawar, Pakistan, in 2003 and 2009, respectively, and the Ph.D. degree from the CECOS University of IT and Emerging Sciences, Peshawar, in 2020. He is currently an Assistant Professor with the CECOS University of IT and Emerging Sciences. His current research interests include motor control and drives, renewable energy, and control of dc/dc power converters.

ANEES ULLAH received the B.Sc. and M.Sc. degrees in electrical engineering from the University of Engineering and Technology, Peshawar, in 2009 and 2011, respectively, and the Ph.D. degree in computer engineering from the Polytechnic University of Turin, Italy, in 2015. From 2016 to 2017, he worked as a Postdoctoral Researcher with the Universidad Antonio de Nebrija, Spain. He is currently working as an Assistant Professor with the Department of Electronics Engineering, University of Engineering and Technology, Peshawar. His research interests include fault-tolerant digital systems design, fault injection in FPGAs, FPGA-based ternary content addressable memories (TCAMs), FPGA-based convolutional neural networks accelerators, and approximate computing.

ALI NASSER ALZAED is currently working with the Department of Architecture Engineering, College of Engineering, Taif University, Taif, Saudi Arabia. He is also working as the Vice President for Planning, Development, and Community Services.